Regulation of bistability in the *std* fimbrial operon of *Salmonella enterica* by DNA adenine methylation and transcription factors HdfR, StdE and StdF

Lucía García-Pastor[1], María A. Sánchez-Romero[1], Marcello Jakomin[1], Elena Puerta-Fernández[1,2,*] and Josep Casadesús [1,*]

[1]Departamento de Genética, Facultad de Biología, Universidad de Sevilla, Apartado 1095, 41080 Sevilla, Spain and [2]Instituto de Recursos Naturales y Agrobiología de Sevilla (IRNAS, CSIC), Avda. Reina Mercedes, 10, 41012 Sevilla, Spain

ABSTRACT

Bistable expression of the *Salmonella enterica std* operon is controlled by an AND logic gate involving three transcriptional activators: the LysR-type factor HdfR and the StdE and StdF regulators encoded by the *std* operon itself. StdE activates transcription of the *hdfR* gene, and StdF activates *std* transcription together with HdfR. Binding of HdfR upstream of the *std* promoter is hindered by methylation of GATC sites located within the upstream activating sequence (UAS). Epigenetic control by Dam methylation thus antagonizes formation of the StdE-StdF-HdfR loop and tilts the *std* switch toward the Std^OFF state. In turn, HdfR binding hinders methylation of the UAS, permitting activation of the StdE-StdF-HdfR loop and concomitant formation of Std^ON cells. Bistability is thus the outcome of competition between DNA adenine methylation and the StdE-StdF-HdfR activator loop.

INTRODUCTION

Fimbriae (pili) are hair-like appendages that permit adhesion to biotic and abiotic surfaces. Such appendages are present in the surface of many Gram-negative bacteria, and have prominent roles in bacterial pathogenesis (1). A canonical fimbrial type includes morphologically diverse fimbriae assembled by the chaperone/usher secretion system (1,2). Pili assembled by this pathway are virulence factors that promote attachment of pathogenic bacteria to host cell surfaces. In addition, chaperone-usher fimbriae may modulate host cell signaling pathways, promote or inhibit bacterial invasion of host cells, and facilitate biofilm formation (1).

Chaperone-usher fimbriae encoded by the *std* operon of *Salmonella enterica* serovar Typhimurium bind a fucosylated receptor present in the mucus of the murine caecum (3). Like other fimbrial loci (4,5), *std* undergoes bistable expression with concomitant formation of Std^ON and Std^OFF subpopulations. Under laboratory conditions, such populations have disparate sizes, >99% Std^OFF cells and <1% Std^ON cells (6). The sizes of Std^ON and Std^OFF subpopulations in the animal intestine remain unknown. However, the observation that mice infected with *S. Typhimurium* seroconvert to StdA, the major fimbrial subunit of Std fimbriae (7), raises the possibility that the Std^ON lineage may become larger during animal colonization.

Expression of the *std* operon is derepressed in mutants lacking DNA adenine (Dam) methylation (8), and constitutive *std* expression attenuates *S. Typhimurium* virulence in a mouse model of acute infection (9). Virulence attenuation, however, is not caused by production of Std fimbriae but by downregulation of pathogenicity island (SPI-1) by two *std*-encoded proteins, StdE and StdF (10). Actually, SPI-1 downregulation is merely an example of the capacity of StdE and StdF to control gene expression: both proteins are transcriptional regulators that act either as repressors or as activators of numerous *S. enterica* genes (6). As a consequence, formation of fimbriae in the Std^ON subpopulation is accompanied by changes in motility, chemotaxis, virulence, biofilm formation and probably in additional phenotypic traits (6). This pleiotropic control is a unique feature among fimbrial operons, and may contribute to adaptation of Std^ON cells to the environment of the large intestine.

In this study, we describe cellular factors and mechanisms that govern bistable expression of the *std* operon. Formation of Std^ON cells requires positive feedback involving three transcriptional regulators (StdE, StdF, and HdfR). In turn, DNA adenine methylation prevents HdfR binding to the *std* UAS, thus permitting formation of Std^OFF cells.

*To whom correspondence should be addressed. Josep Casadesús. Tel: +34 95 455 7105; Email: casadesus@us.es
Correspondence may also be addressed to Elena Puerta-Fernández. Tel: +34 95 455 3822; Email: elena.puerta@irnas.csic.es

MATERIALS AND METHODS

Bacterial strains, bacteriophages and strain construction

Salmonella enterica strains listed in Supplementary Table S1 belong to serovar Typhimurium and derive from the mouse-virulent strain SL1344 (11). For simplicity, *S. enterica* serovar Typhimurium is often abbreviated as *S. enterica*. *Escherichia coli* BL21 [F⁻ *dcm ompT hsdS* (rB⁻ mB⁻) *gal* [malB⁺]K12(λS)] (Stratagene, La Jolla, CA, USA) was used for protein purification. Targeted gene disruption was achieved using plasmids pKD3, pKD4 or pKD13 as templates to generate polymerase chain reaction (PCR) products for homologous recombination (12). Antibiotic resistance cassettes introduced during strain construction were excised by recombination with plasmid pCP20 (12). Primers used in strain construction are shown in Supplementary Table S2. Transductional crosses using phage P22 HT 105/1 *int201* (13) were used for strain construction operations involving chromosomal markers. The transduction protocol has been previously described (14). To obtain phage-free isolates, transductants were purified by streaking on green plates. Phage sensitivity was tested by cross-streaking with the clear-plaque mutant P22 H5.

Construction of strain SV9322 (P$_{LtetO}$-*stdEF stdA::gfp*) was achieved by insertion of the P$_{LtetO}$ promoter upstream of *stdE* on the *Salmonella* chromosome. For this purpose, the P$_{LtetO}$ promoter (including a kanamycin resistance [Km^R] cassette linked to the P$_{LtetO}$ promoter) was amplified from SV7553 (6), using the oligonucleotides *PLtetOstdEF pStd UP* and *PLtetOstdEF pStd DO* and the PCR product used for homologous recombination. For verification of correct chromosomal insertion, primers *PLtetO sense* and *stdE E2* were used.

Strain SV8449 (P$_{LtetO}$*hdfR*) harbors the P$_{LtetO}$ promoter upstream the *hdfR* coding sequence on the *S. enterica* chromosome. To construct this strain, the P$_{LtetO}$ promoter was amplified from SV7553 (6) with oligos *PLtetOhdfR UP* and *PLtetOhdfR DO*. The resulting PCR product was integrated into the chromosome of *S. enterica*. The Km^R cassette introduced during construction was excised by recombination with plasmid pCP20 (12). For verification of correct chromosomal insertion, primers *PLtetO sense* and *hdfR E2* were used.

Media and growth conditions

Bertani's lysogeny broth (LB) (15) was used as standard rich medium. Solid LB contained agar at 1.5% final concentration. Cultures were grown at 37°C. Aeration of liquid cultures was obtained by shaking at 200 rpm in an Infors Multitron shaker. 5-bromo-4-chloro-3-indolyl-β-D-galactopyranoside ('X-gal', Sigma-Aldrich) was used as chromogenic indicator of as indicator of β-galactosidase activity. Antibiotics were used at the final concentrations described elsewhere (16).

Genetic screen

Strain SV8188 (*stdA::lacZ*) was transduced with nine pools of a *S. enterica* pBR328 plasmid library (10). Each pool contained around 1000 independent clones. Transductants were selected on LB supplemented with ampicillin. Candidates that retained high β-galactosidase activity after re-transformation were further analyzed. The DNA fragments contained in the plasmids of selected candidates were sequenced using specific primers flanking the insertion site (Supplementary Table S2).

β-galactosidase assays

Levels of β-galactosidase activity were determined using the CHCl₃-sodium dodecyl sulfate permeabilization procedure (17). β-galactosidase activity data (Miller units) are averages and standard deviations from ≥3 independent experiments.

Flow cytometry analysis

Bacterial cultures were grown at 37°C in LB until stationary phase (OD$_{600}$≅2). Cells were then diluted in phosphate-buffered saline (PBS) to a final concentration of ∼10⁷ cells/ml. Data acquisition was performed using a Cytomics FC500-MPL cytometer (Beckman Coulter, Brea, CA, USA). Data were collected for 100 000 events per sample and were analysed with CXP and FlowJo 8.7 softwares. Data are shown by dot plots representing forward scatter (cell size) in the *y*-axis versus fluorescence intensity in the *x*-axis.

In vivo visualization of *std*-expressing cells

For time-lapse microscopy, strains containing the *stdA::gfp* fusion in wild-type and P$_{LtetO}$*hdfR* backgrounds (SV9597 and SV9292, respectively) were grown overnight at 37°C in LB and diluted 1:100 in fresh medium. Cultures were grown to the desired optical density and concentrated 10-fold by centrifugation at 8000 *g* for 5 min. Cells were placed on an agarose slab (0.8% agarose/1% LB) and warmed to 37°C. Images were captured with a Zeiss Apotome fluorescence microscopy equipped with a 100× Plan Apochromat objective and an incubation system that permits observation and cultivation of living cells. Pictures were taken at different times using an Axiocam 506 camera, and the images were analyzed using ImageJ software (Wayne Rasband, Research Services Branch, National Institute of Mental Health).

Purification of HdfR-His₆

The *S.* Typhimurium *hdfR* gene was PCR-amplified using primers *hdfR*-NheI *FOR* and *hdfR*-EcoRI *REV*, and cloned onto the NheI and EcoRI restriction sites of pET-21a[+] (Novagen). The GTG start codon of *hdfR* was replaced with the ATG start codon of the vector. The resulting plasmid, pIZ1803, allows expression of the *hdfR* gene from the T7 promoter, and the HdfR protein harbors a 6xHis tag at the C-terminus. For purification of HdfR-His₆, *E. coli* strain BL-21 was transformed with pIZ1803 and grown at 37°C in LB. Gene expression was induced with 1 mM IPTG, added when cells reached an OD$_{600}$ ≅ 0.5. After IPTG addition, cells were grown for 2 h. For lysis, bacteria were sonicated in lysis buffer (30 mM Tris HCl pH 7, 2 M NaCl). HdfR-His₆ protein was purified from the cell-free extract on HIS-Select® Nickel Affinity Gel (Sigma-Aldrich), treated with

washing buffer (30 mM Tris–HCl pH 7, 2M NaCl, 10 mM imidazole) and eluted with elution buffer (30 mM Tris–HCl pH 7, 2 M NaCl, 200 mM imidazole). At last, the protein was dialyzed using a dialysis tubing cellulose membrane, 10 × 6 mm (Sigma-Aldrich) in lysis buffer to eliminate imidazole.

Electrophoretic mobility shift assays (EMSA)

An *std* promoter probe labeled with 6-caroxyfluorescein (6-FAM) was prepared by PCR amplification of a 306 bp region containing the *std* promoter (-295 to $+11$), using 5′-labeled oligonucleotide *std EMSA-6FAM FOR* and non-labeled *std EMSA REV.* A 'cold' DNA probe was prepared using the same primers without 6-FAM label. For Electrophoretic mobility shift assays (EMSA) with methylated DNA, the 6-FAM labeled probe was methylated *in vitro* using Dam methylase (New England Biolabs), and digested with *Mbo*I (New England Biolabs) to discard nonmethylated DNA. The undigested product was purified with the Wizard® SV Gel and PCR clean-up system (Promega). For a standard binding reaction, 50 ng of DNA probe, 1 μg of poly[d(I-C)] (Roche, Penzberg, Germany) and different amounts of purified HdfR-His$_6$ were mixed to yield 20 μl final volume. The binding buffer contained 50 mM KCl, 20 mM Tris–Cl (pH 8), 1 mM dithiothreitol, 10% glycerol and bovine serum albumin 150 μg/ml. The mixture was stored at 4°C for 20 min. As a negative control, a competition assay with excess of 'cold' DNA fragment was performed using 500 ng of purified HdfR-His$_6$ and 50 ng FAM-labeled *stdA* promoter probe. Increasing amounts of 'cold' stdA promoter probe from 0 to 1000 ng were tested. DNA–protein complexes were subjected to electrophoresis at 4°C in a 5% non-denaturing acrylamide/bisacrylamide (29:1) gel prepared in Tris-glycine buffer (25 mM trizma base, 190 mM glycine, 1 mM ethylenediaminetetraacetic acid (EDTA)). DNA fragments were visualized with a FLA-5100 Imaging system (Fujifilm, Tokyo, Japan).

Chromatin Immunoprecipitation followed by sequencing (ChIP-seq) and data analysis

Strain SV9287 (P$_{LtetO}$-*stdEF::*3xFLAG) was used to perform ChIP-seq experiments, and the protocol was described elsewhere (6). ChIP DNA samples were sequenced at the Functional Genomics Core Facility of the Institute for Research in Biomedicine, Barcelona (Spain) using Illumina's sequencing technology. BAM files were converted to FASTQ format with the BAM2FASTQ tool (http://www.hudsonalpha.org/gsl/information/software/bam2fastq).The quality of the sequence reads was examined using FASTQC (18). The adapters were trimmed with the FASTX_CLIPPER tool of the FASTX-Toolkit suite (http://hannonlab.cshl.edu/fastx_toolkit/). Reads shorter than 40 nt were discarded. NCBI GCA_000210855.2 genome assembly of *S. enterica* SL1344 was used as reference genome. Mapping was performed with Bowtie (19) allowing two-mismatches for only unique alignment. Peaks were called using CisGenome version 2.0 (20) using default parameters. The IGV browser (21) was used for data visualization. Genes closest to a ChIP peak were identified using the bedtools suite (22).

Chromatin immunoprecipitation coupled to quantitative PCR (ChIP- qPCR)

ChIP-qPCR assays were used to test StdE, StdF and HdfR binding to the *std* promoter region. The strains used were SV9324 (Δ*dam stdE*-3xFLAG), SV9325 (Δ*dam stdEF*-3xFLAG), SV9287 (P$_{LtetO}$*stdEF*-3xFLAG), SV9766 (P$_{LtetO}$*stdEF*-3xFLAG Δ35nt), SV8487 *(Δdam hdfR*-3xFLAG) and SV8504 *(hdfR*-3xFLAG). The chromatin immunoprecipitation (ChIP) protocol used was described previously (6). After DNA purification, quantitative PCR was performed in a Light Cycler 480 II apparatus (Roche). Each reaction was carried out on a 480-well optical reaction plate (Roche) in a total volumen of 10 μl, containing 5 μl SYBR mix, 0.2 μl DYE II (Takara), 4 μl DNA and two gene-specific primers (0.2mM), named RT-promoter std FOR and RT-promoter std REV, listed in Supplementary Table S2, for amplification of the *std* promoter region in both IP sample and mock IP simple. Real-time cycling conditions were as follows: (i) 95°C for 10 min and (ii) 40 cycles at 95°C for 15 s, 60°C for 1 min. Triplicates were run for each reaction, and the Ct value is averaged from them. Absence of primer dimers was corroborated by running a dissociation curve at the end of each experiment to determine the melting temperature of the amplicon. Melting curve analysis verified that each reaction contained a single PCR product. For quantification, the efficiency of each primer pair was determined to be between 90%-110%, following the instructions for efficiency determination described in the 'Guide to Performing Relative Quantification of Gene Expression Using Real-Time Quantitative PCR' (Applied Biosystems). These efficiencies indicate that the amount of DNA is doubled in each PCR cycle, and allows for direct comparison between different genes. Relative RNA levels were determined using the ΔΔCt method as described in the above mentioned guide. Briefly, each gene *Ct* value is normalized to the *Ct* value for the internal control (*rfaH*), which gives the ΔCt value. This value is then related to a given gene in the reference strain (*S. enterica*, in this case) giving us the ΔΔCt value. Since the amount of DNA doubles in each PCR cycle, the relative amount of input cDNA can be determined by using the formula 2-ΔΔCt. Each ΔΔCt determination was performed at least in three different DNA samples (three biological replicates), and the results are representative example of such determinations.

Southern blotting

Genomic DNA was isolated by phenol extraction and ethanol precipitation from stationary cultures in LB (O.D.$_{600} \cong 2$). Forty μg of each DNA sample was digested with *Ssp*I (New England Biolabs), purified and divided into four fractions, three of which were subsequently digested with *Dpn*I, *Mbo*I or *Sau*3AI (New England Biolabs). After digestion the samples were run in a denaturing 8% TBE (tris-borate-EDTA)-polyacrilamide (19:1), 8 M urea gel. Electrophoresis was carried out in a Hoefer SE400 (Hoefer Scientific Instruments) apparatus subjected to an electric field of 35 mA for 60 min. After electroforesis, DNA was transferred to an Amersham Hybond-N+ membrane (GE Healthcare, Wauwatosa, WI, USA), using a semidry

Electroblotting system (Thermo Scientific) (400mA, 5V, 3 h). The DNA in the membrane was immobilized by UV crosslinking. A radioactive probe was prepared by PCR using α-^{32}P labeled dCTP (Perkin Elmer) and oligonucleotides *std PLtetO UP* and *std southern DO*. After the PCR reaction, non-incorporated nucleotides were removed using a Sephadex G-25 column (Illustra MicroSpin G-25 columns, GE Healthcare) following manufacturer's instructions. Prior to hybridization the double-stranded DNA probe was denatured by heating at 95°C for 3 min, followed by incubation on ice. Hybridization with the probe was performed overnight at 52°C in hybridization buffer (0.5 M sodium phosphate pH 7.2, 10 mM EDTA, 7% sodium dodecyl sulphate (SDS)). Excess probe was removed with washing buffer (40 mM sodium phosphate pH 7.2, 1% SDS) at 48°C (three washes, 30 min each). The membrane was developed using a FLA-5100 Scanner (Fujifilm).

Site-directed mutagenesis

Mutation of the three GATC sites contained in the promoter region of the *std* promoter was achieved using the QuikChange® Site-Directed Mutagenesis Kit (Stratagene). Briefly, a 1 Kb fragment of the *std* promoter region containing the three GATC sites was cloned into the pGEMT plasmid using the oligonucleotides Std-promoter-XbaI and Std-promoter-SacI. Mutations in every GATC were then introduced using oligonucleotides harboring GATC changes (labeled as mut For and mut Rev). Resulting plasmids containing fragments with changes in the GATC sites were then digested with *Xba*I and *Sac*I, cloned onto the suicide plasmid pDMS197 (23) and propagated in *E. coli* CC118 lambda *pir*. Plasmids derived from pMDS197 were transformed into *E. coli* S17–1 lambda *pir*. The resulting strains were used as donors in matings with *Salmonella* cells harboring a Cm^R cassette in place of the three GATC sites (constructed using oligonucleotides Mut std promoter P1 and Mut std promoter P2) as recipients. Tc^R transconjugants were selected on E plates supplemented with tetracycline. Several Tc^R transconjugants were grown in nutrient broth (without NaCl) containing 5% sucrose. Individual tetracycline-sensitive segregants were then screened for cloramphenicol sensitivity and examined for the incorporation of the mutant allele by *Sau*3AI digestion and DNA sequencing using external oligonucleotides.

Dam methylation protection assay

A 306 bp DNA fragment was PCR-amplified from genomic DNA of strain SV6024 (containing a CATC sequence instead of GATC-1 at the *std* UAS). HdfR-His$_6$ was pre-bound to *std* DNA by incubation at 4°C for 20 min. Dam methylase (8 U) and S-adenosyl-methione (160 mM) prepared in 20 μl Dam methylase buffer were added. The DNA methylation reaction was allowed to proceed at 37°C for 2 h. To determine the extent of DNA binding, 10 μl was removed and run as an EMSA. The remainder of the reaction was incubated at 65°C for 20 min to dissociate bound HdfR-His$_6$ from the DNA and to inactivate Dam methylase. The DNA was finally digested with *Dpn*I at 37°C for 1 h, and digestion products were resolved on an agarose 2% gel.

Magnetic activated cell sorting (MACS)

A 500 ml aliquot from a stationary culture (OD$_{600}$≅2) of strain SV9602 (P$_{LtetO}$-*hdfR stdA*::3xFLAG) was collected by centrifugation. The pellet was washed with 10 ml of TE buffer and fixed by adding the same volume of cold 70% ethanol. Ethanol-fixed cells were washed three times with PBS containing 0.05% of Tween (PBS-T). The pellet was resuspended in 5 ml of lysozyme solution (2 mg/ml lysozyme, 25 mM Tris–HCl pH 8.0, 50 mM glucose and 10 mM EDTA) and incubated at room temperature for 10 min. Cells were then washed three times with PBS-T and incubated for 30 min in 10 ml of 2% BSA in PBS-T. Cells were centrifuged and incubated 1 h at RT with anti-flag-PE antibody (Miltenyi). After incubation, cells were washed with PBS-T. Cells were then incubated overnight at 4°C with anti-PE microbeads (Miltenyi) and washed with PBS-T. Separation of labeled and unlabeled cells was performed using an autoMACS Pro Separator (Miltenyi).

Analysis of GATC methylation by PCR

Genomic DNA was isolated by phenol extraction and ethanol precipitation from Std^{OFF} and Std^{ON} magnetic-activated sorted cells of strain SV9602. A total of 70 ng of each DNA sample were digested with the endonucleases *Dpn*I and *Mbo*I (New England Biolabs). After digestion, RT-PCR was performed using the samples as templates. *EMSA std* and *std southern DO* oligonucleotides were used (Supplementary Table S2).

RESULTS

Genetic screen for activators of *std* expression

To search for factors that might activate expression of the *std* operon, a genetic screen was performed using a pBR328-based library containing 7–11 kb segments of the *S. enterica* genome (10). A strain carrying a *stdA*::*lacZ* translational fusion (SV8188) was used as reporter. This strain is Lac$^−$ on X-gal agar as a consequence of the small size of the Std^{ON} subpopulation (6). Strain SV8188 was transduced with nine pools of the plasmid library, each containing around 1000 independent clones. Forty-five colonies with increased β-galactosidase activity (blue) were chosen, and 22 independent candidates that retained high β-galactosidase activity after re-transformation of their plasmid were further analyzed. The DNA fragments contained in 15 candidate plasmids were sequenced using primers flanking the insertion site (Supplementary Table S1). Somehow surprisingly, 14 plasmids turned out to carry the *std* gene cluster as well as heterogeneous assortments of neighbouring genes. One such plasmid (pBR328 *std*) was propagated as pIZ2318. These observations indicated that activators of the *std* operon are contained within the operon itself (Figure 1A).

A candidate that formed faint blue colonies turned out to contain an incomplete *std* fimbrial operon lacking the downstream 21 nt of the *stdE* coding sequence and the entire *stdF* gene (pBR328 *std*Δ21*stdE*-Δ*stdF*, propagated as pIZ2319) (Figure 1A). β-galactosidase analysis confirmed that *stdA::lacZ* expression decreased when *stdE* contained
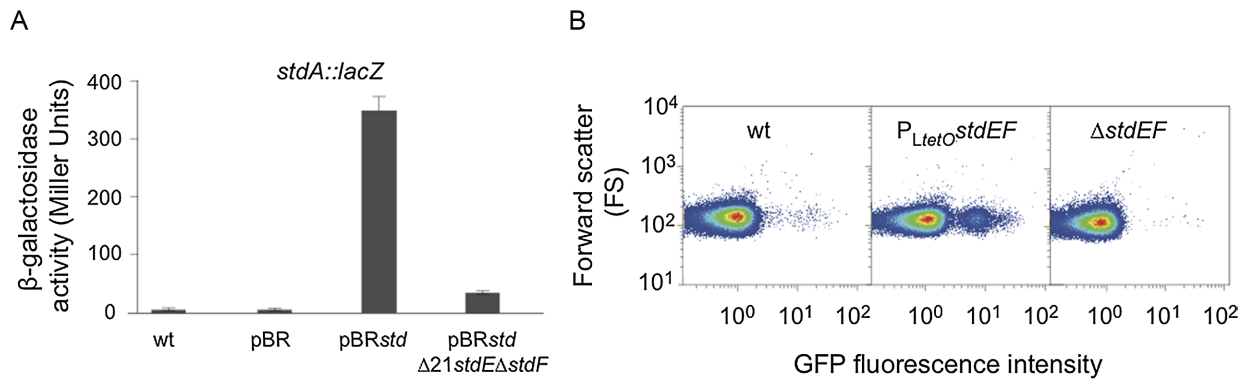
A

B

Figure 1. Autogenous regulation of the *std* operon by StdEF. (**A**) β-galactosidase activity of a *stdA::lacZ* fusion in the presence of plasmid containing either the entire *std* operon or a deletion of *stdE* and *stdF*. Numbers (Miller units) are averages and standard deviations from 3 experiments. (**B**) Flow cytometry analysis of *stdA::gfp* expression in a wild-type background, in a strain that constitutively expresses StdE and StdF, and in a strain carrying an *stdEF* deletion.

a downstream deletion and the *stdF* gene was absent (Figure 1A). These observations suggested that StdE and StdF, previously shown to act as global regulators of gene transcription (6), might also be involved in autogenous control of *std* transcription. This hypothesis was confirmed upon constitutive expression of StdE and StdF, using a strain (SV9322) that harbors an *stdA::gfp* transcriptional fusion and *stdEF* expression driven by the heterologous constitutive promoter P_{LtetO} (24,25), placed upstream of *stdEF*. Single cell analysis of *stdA::gfp* expression was monitored by flow cytometry, and a representative experiment is shown in Figure 1B. Constitutive transcription of *stdEF* increased the size of the Std^ON subpopulation, and deletion of *stdEF* resulted in loss of Std^ON cells. Hence, formation of the Std^ON lineage does require transcriptional activation by StdE and/or StdF.

Transcriptional activation of *std* by StdF

ChIP followed by sequencing (ChIP-seq) revealed the existence of an StdF binding site upstream of the *stdA* promoter (Figure 2A). The existence of this site was further tested using ChIP coupled with quantitative PCR (ChIP-qPCR). Because Dam methylation represses *std* transcription (9), the trial was performed in a Dam⁻ strain. A chromatin fragment containing the *std* promoter immunoprecipitated with StdF-3xFLAG was found to be enriched 6 times compared with the mock immunoprecipitated sample (Figure 2B), confirming that StdF binds upstream of the *std* promoter *in vivo*. No binding was observed for StdE. In turn, StdF failed to bind when a strain containing a deletion upstream of the *std* promoter (from −338 to −303) was subjected to ChIP-qPCR (Figure 2C), thus confirming the existence of the StdF binding site identified by ChIP-seq. These observations, together with the existence of autogenous positive control (Figure 1), provide evidence that StdF directly activates *std* transcription.

Transcriptional activation of *hdfR* by StdE

In a previous study, the *hdfR* gene was found to be upregulated upon constitutive expression of *stdEF* (6), suggesting

that StdE and/or StdF might activate *hdfR* transcription. β-galactosidase analysis using a translational *hdfR::lacZ* fusion (strain SV7889) provided evidence that StdE alone is sufficient to activate *hdfR* transcription (Figure 3A). Furthermore, ChIP-seq analysis identified an StdE binding site upstream of the *hdfR* gene (Figure 3B). StdF binding was not detected, thus providing futher evidence that the transcriptional activator of *hdfR* is StdE only.

Because HdfR is a LysR-type transcriptional regulator and LysR-like factors often repress their own expression (26), we cloned a 260 bp DNA fragment that contained the putative *hdfR* promoter as well as upstream and dowstream regions (from −160 to +100) on the promoter-probe vector pIC552 (27). The resulting plasmid (pIZ2320) thus harbored a $P_{hdfR}::lacZY$ transcriptional fusion. The activity of the fusion was monitored in HdfR⁺ and HdfR⁻ strains, and decreased activity in the HdfR⁺ background provided evidence that HdfR undergoes autogenous transcriptional repression (Figure 3C).

Transcriptional activation of *std* by HdfR

Because a previous study had identified HdfR as an activator of the *std* operon (9), we examined whether formation of the Std^ON lineage was HdfR dependent. For this purpose, we placed *hdfR* under the control of the heterologous, constitutive promoter P_{LtetO}(24,25). In the construct, the native *hdfR* promoter was removed, thus avoiding autogenous control (strain SV8449). Transcription of the *std* operon was then examined using *stdA::lacZ* and *stdA::gfp* fusions (strains SV8477 and SV9292, respectively). Analysis of β-galactosidase activity and flow cytometry assessment of *stdA::gfp* expression showed that constitutive *hdfR* transcription upregulates *stdA::lacZ* expression (Figure 4A) and increases the size of the Std^ON subpopulation (Figure 4B, upper panel). The latter observation was made not only by flow cytometry but also on X-gal plates, where Lac⁺ (Std^ON) and Lac⁻ (Std^OFF) colonies were observed in strain SV8477 ($P_{LtetO}hdfR$ *stdA::lacZ*) but not in SV8188 (*stdA::lacZ*) (Figure 4C). Formation of the Std^ON subpopulation thus requires both StdEF and HdfR (Figure 4B, lower panel), suggesting the existence of a network of posi-
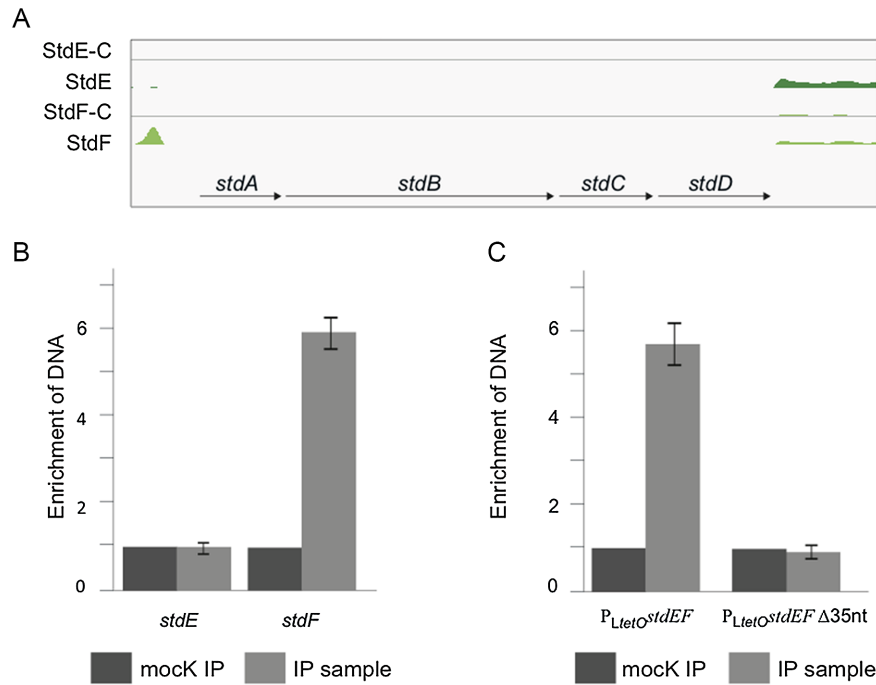
Figure 2. Binding of StdF to the *std* promoter. (**A**) ChIP-seq analysis of StdE and StdF binding to the *std* UAS. StdE-C and StdF-C are mock immunoprecipitated samples. (**B**) *In vivo* analysis of StdE and StdF binding to the *std* UAS by ChIP coupled with quantitative PCR. The experiment was performed in a Dam⁻ background. (**C**) *In vivo* analysis of StdF binding to wild-type and deleted versions of *std* UAS using ChIP coupled with quantitative PCR. The strain carrying the P$_{LtetO}$*stdEF*-3xFLAG Δ35nt construct lacks the Std binding site. In B and C, data are averages and standard deviations from three independent experiments.
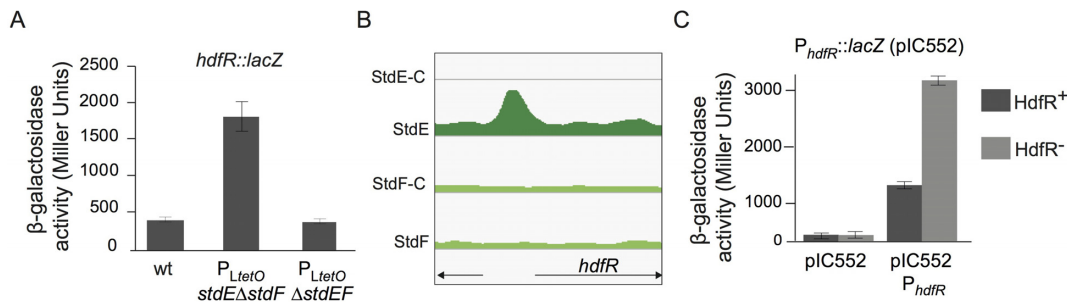
Figure 3. Regulation of *hdfR* transcription by StdE. (**A**) β-galactosidase activity of a *hdfR::lacZ* transcriptional fusion in the presence and in the absence of StdE. (**B**) ChIP-seq analysis of StdE and StdF binding upstream of the *hdfR* gene. StdE-C and StdF-C are mock immunoprecipitated samples. (**C**) β-galactosidase driven by the *hdfR* promoter in the presence and in the absence of HdfR.

tive feedback: StdF and HdfR activate *std* transcription and StdE activates *hdfR* transcription.

Role of positive StdE-StdF-HdfR feedback in the stability of the Std^{ON} state

The observation that constitutive transcription of *hdfR* yields Lac⁺ and Lac⁻ colonies on X-gal plates raised the possibility that activation of StdE-StdF-HdfR feedback above a critical threshold might increase the stability of the Std^{ON} state making it heritable. Note that a previous study using the same *stdA::lacZ* fusion had failed to detect Lac⁺ (Std^{ON}) colonies on X-gal plates, and had explained the absence of Lac⁺ colonies as a consequence of the instability (and concomitant small size) of the Std^{ON} subpopulation (6). The effect of StdE-StdF-HdfR feedback activation on

the stability of Std^{ON} state was examined by time lapse experiments, monitoring expression of an *stdA::gfp* fusion in a wild-type background (strain SV9597) and in a strain that carried an P$_{LtetO}$*hdfR* construct (SV9292). The results of these experiments were clear-cut: (i) cells expressing a native level of HdfR failed to transmit the Std^{ON} state to daughter cells (Figure 5A); (ii) in contrast, among cells with increased HdfR level, a fraction was found to transmit the Std^{ON} state to the progeny (Figure 5B). Hence, the small size of the Std^{ON} population in a wild-type background (6) appears to be caused indeed by quick return to the Std^{OFF} state upon cell division. This view was confirmed by fluorescence microscopy: Std^{ON} cells did not produce Std^{ON} progeny (Figure 5C) unless HdfR expression increased (Figure 5D). The latter observation is in agreement with the
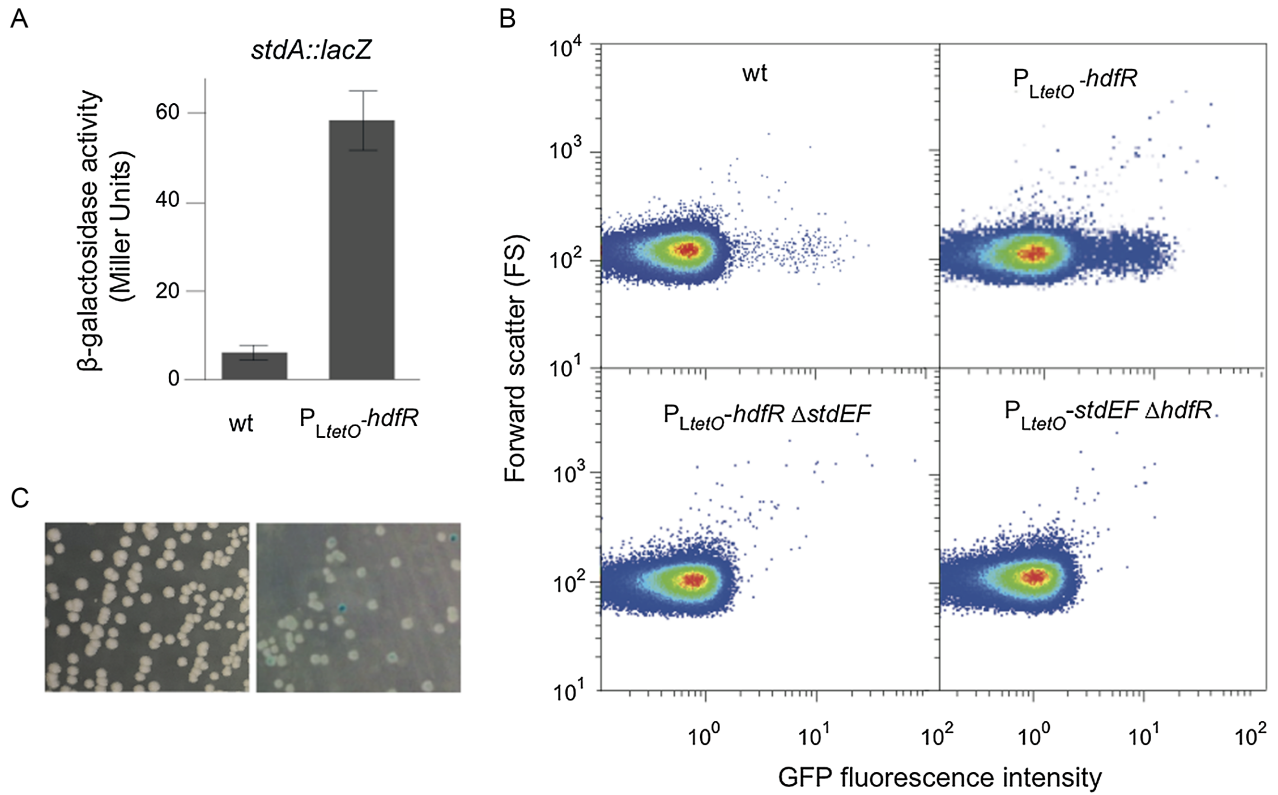
Figure 4. Role of HdfR in *std* transcription. (**A**) β-galactosidase activity of an *std::lacZ* transcriptional fusion in the wild-type and in a strain that constitutively expresses hdfR (P$_{LtetO}$hdfR). (**B**) Flow cytometry analysis of expression of an *stdA::gfp* transcriptional fusion in the wild-type and upon constitutive expression of either HdfR or StdEF. (**C**) Formation of Lac$^-$ colonies on X-gal plates by the wild-type (left panel). Formation of Lac$^+$ and Lac$^-$ colonies by a strain carrying an *stdA::lacZ* transcriptional fusion in a P$_{LtetO}$hdfR background (right panel).
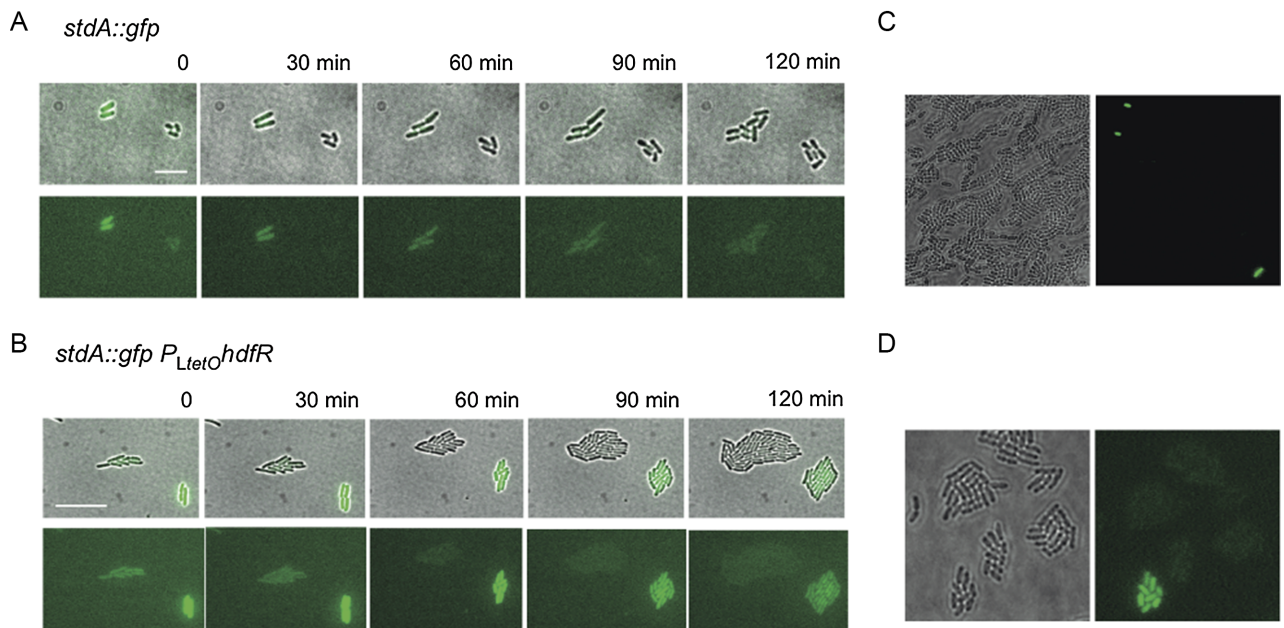

Figure 5. Heritability of the Std^{ON} state. (**A**) Time lapse (120 min) microscopy observation of *Salmonella enterica* cells carrying an *stdA::gfp* transcriptional fusion. The upper panel shows the bright field merged with the *gfp* channel while the bottom panel shows the *gfp* channel only. (**B**) Time lapse (120 min) microscopy observation of *S. enterica* cells carrying an *stdA::gfp* transcriptional fusion in a P$_{LtetO}$hdfR background. Panels are as above. (**C**) Absence of fluorescent microcolonies due to instability of the Std^{ON} state. (**D**) Inheritance of the Std^{ON} state and formation of a fluorescent microcolony.

formation of Lac⁺ colonies upon constitutive synthesis of HdfR (Figure 4C).

Binding of HdfR to the *std* upstream activating sequence (UAS)

The finding that HdfR activates *std* transcription prompted the examination of HdfR binding to the *std* promoter region *in vitro.* For this purpose, we used a 306 bp DNA fragment containing *std* DNA from −295 to +11. The fragment included the *std* promoter and the transcription start site (9). Binding of HdfR to the fragment was assayed using purified HdfR-His$_6$ protein. Complementation of an *hdfR* mutation by HdfR-His$_6$ indicated that this protein is functional (Supplementary Figure S1). Electrophoretic mobility shift assays (EMSA) showed that 500 ng of HdfR-His$_6$ was able to retard 50 ng of *stdA* FAM-labeled probe (Figure 6A). HdfR binding to the *std* UAS was thus confirmed.

The *std* UAS contains three GATC sites in a 25 bp interval, at positions −242 (GATC-1), −229 (GATC-2) and −220 (GATC-3) (9). Because *std* transcription is derepressed in Dam⁻ mutants (8,9), we considered the possibility that the interaction between HdfR and the *std* promoter might be dependent on the DNA methylation state of the UAS. For this purpose, EMSA was performed using a methylated version of the FAM-labeled probe described above. HdfR-His$_6$ failed to bind the methylated *std* probe *in vitro* (Figure 6A). Binding of HdfR-His$_6$ was reduced when 'cold' competitor DNA was added to the binding reaction (Figure 6B).

The effect of DNA adenine methylation on HdfR binding to the *std* UAS was also investigated *in vivo*, using ChIP coupled with quantitative PCR. Strains SV8504 (*hdfR*-3xFLAG) and SV8487 (Δ*dam hdfR*-3xFLAG) were used. In the Dam⁻ strain, a chromatin fragment containing the *std* promoter was 13-fold enriched in the inmunoprecipitated (IP) sample compared with the mock IP sample (Figure 6C). However no enrichment was detected in the Dam⁺ strain (Figure 6C). *In vitro* and *in vivo* analyses thus confirm that HdfR binding to the *std* UAS is hindered by DNA adenine methylation, and explain why derepression of the *std* operon is observed in a Dam⁻ background (8,9).

Site-directed mutagenesis of the *std* UAS

To investigate whether the GATC-1, GATC-2 and GATC-3 sites were located in the region bound by HdfR in the *std* UAS, individual GATC sites were subjected to site-directed mutagenesis. Two types of nucleotide substitutions were introduced: GATC → GTTC, and GATC → GATG. A strain that lacked all three GATC sites was also constructed. The effect of nucleotide substitutions on *std* expression was monitored by quantitative RT-PCR. Because the operon is repressed in the wild-type, the experiments were performed in a Dam⁻ background. The results can be summarized as follows:

(i) Site-directed mutagenesis of GATC-1 permitted *std* expression, irrespectively of the nucleotide substitution introduced (GATC → GTTC or GATC → GATG). This observation suggests that GATC-1 may not be

part of the HdfR binding site, thus making unlikely that GATC-1 methylation may participate in *std* repression.

(ii) Site-directed mutagenesis of either GATC-2 or GATC-3 abolished *std* expression in a Dam⁻ background (Figure 7). A tentative explanation may be that GATC-2 and GATC-3 are both part of the HdfR binding site, which is destroyed by GATC → GTTC and GATC → GATG nucleotide substitutions. If this view is correct, it is not surprising that site-directed mutagenesis of all three GATC sites, converting them to either GTTC or GATG, abolished *std* expression in a Dam⁻ background (Figure 7A.).

The above conclusions were supported by EMSA analysis of HdfR binding to FAM-labeled *std* fragments lacking specific GATC sites. A GATC → GATG mutation in GATC-1 did not prevent HdfR binding, while the same mutation in either GATC-2 or GATC-3 completely abolished binding (Figure 7B).

Dam methylation protection by HdfR

Binding of proteins to DNA containing GATC sites can result in methylation hindrance, thus yielding undermethylated DNA (28). To determine whether binding of HdfR to the *std* UAS can prevent DNA methylase activity *in vitro*, we examined whether the Dam enzyme was able to methylate GATC-2 and GATC-3 after HdfR binding. GATC methylation was tested by restriction analysis with *Dpn*I, which cuts methylated DNA only. To simplify restriction analysis, the 'uninteresting' GATC-1 was excluded from the trial. A 306 bp DNA fragment was PCR amplified from genomic DNA of strain SV6024 (carrying a CATC sequence instead of GATC-1). HdfR-His6 was bound to *std* DNA, and *in vitro* methylation by Dam methylase was tested. The conclusion from these experiments was unambiguous: HdfR did protect GATC-2 and GATC-3 from Dam methylation *in vitro* (Figure 8).

Methylation state of the *std* UAS *in vivo*

If the conclusion that HdfR is unable to bind a methylated *std* UAS is correct, one may predict that the GATC sites located within the HdfR binding site must be methylated in Std^{OFF} cells and nonmethylated in Std^{ON} cells. This prediction was first tested in the wild-type, where Std^{OFF} cells represent >99% of the population (6). A control was simultaneously performed using genomic DNA from a Dam⁻ strain (SV5367). The methylation state of individual GATC sites was inferred from Southern blot analysis using enzymes that cut GATC sequences depending on their methylation state (*Mbo*I, *Dpn*I and *Sau*3AI). All three GATC sites within the *std* UAS were found to be methylated in the wild-type (Figure 9A).

Because Southern blot analysis cannot be applied to the Std^{ON} cell lineage due to small size (6), Std^{ON} and Std^{OFF} cell lineages were separated by magnetic activated cell sorting (MACS) using a strain that expressed *hdfR* under the control of the P$_{LtetO}$ promoter (SV9602). Genomic DNAs were digested with *Mbo*I, which cuts nonmethylated DNA and DpnI, which cuts methylated DNA. The methylation
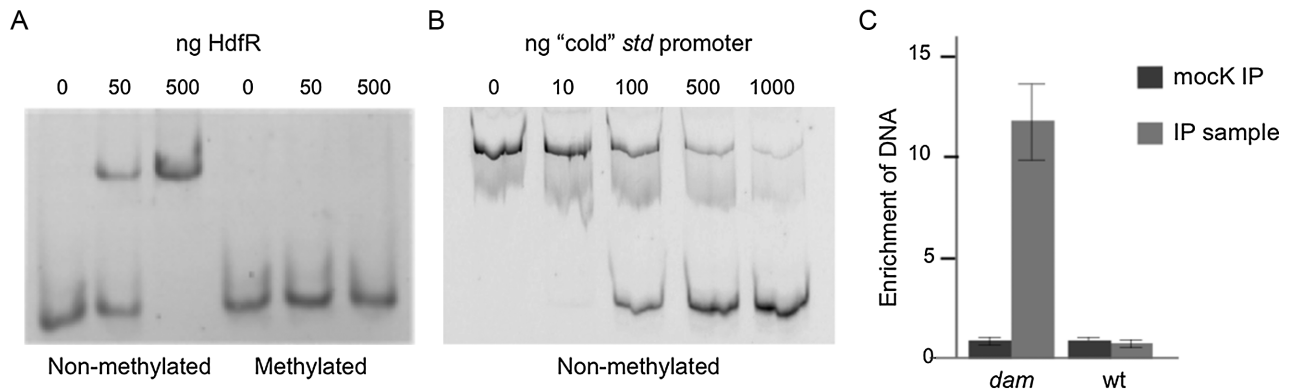
Figure 6. Binding of HdfR to the *std* promoter *in vitro* and *in vivo*. (**A**) Electrophoretic mobility shift assay performed with increasing amounts of purified HdfR-His$_6$ and methylated and nonmethylated versions of a FAM-labeled *stdA* promoter probe. (**B**) Competition assay with excess of 'cold' DNA fragment. (**C**) *In vivo* analysis of HdfR binding to the *std* UAS by ChIP coupled with quantitative PCR. The experiment was performed in Dam$^+$ and Dam$^-$ backgrounds. Data are averages and standard deviations from three independent experiments.
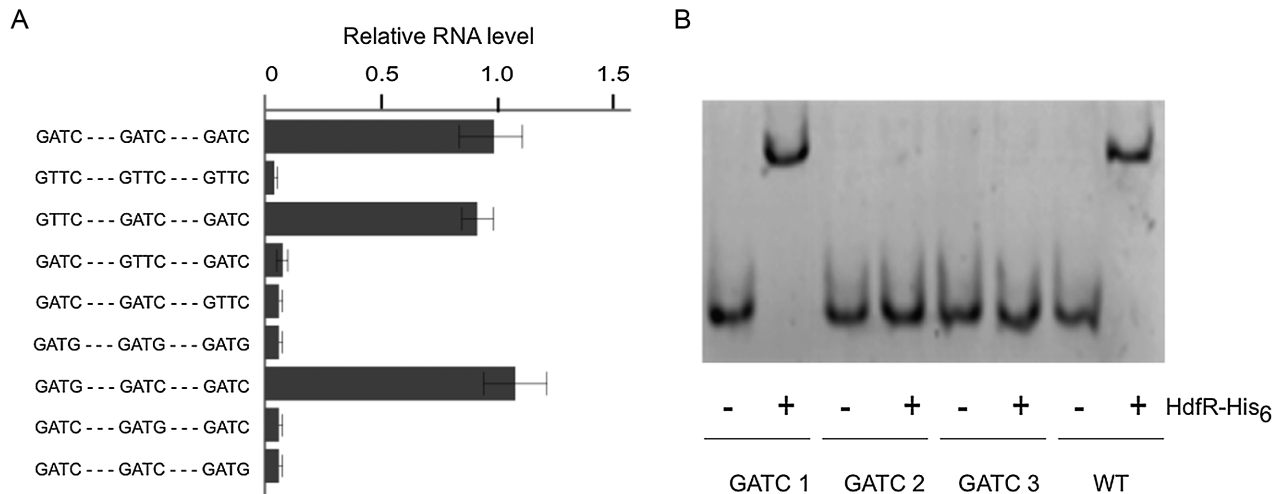
Figure 7. Role of individual GATC sites within the *std* UAS in transcriptional control. GATC-1 is the promoter-distal site, GATC-2 is the central site and GATC-3 is the promoter-proximal site. (**A**) Relative amounts of *std* mRNA transcribed from the *stdA* promoter in strains harboring one or more mutations in the GATC sites of the *std* UAS. Absolute data obtained with quantitative real-time PCR were normalized to the RNA content of the Dam$^-$ strain. Data are averages and standard deviations from five independent experiments. (**B**) EMSA analysis performed without HdfR (−) or with 500 ng of purified HdfR-His$_6$ (+). Binding assays employed FAM-labeled *std* promoter probes carrying mutations in GATC-1, GATC-2 and GATC-3. A FAM-labeled *std* fragment containing the wild-type sequence was included as a positive control.

state of the *std* UAS was determined by quantitative PCR. A delay in amplification compared with non-digested DNA indicated digestion. Results were as follows:

(i) DNA from Std^{OFF} cells (Figure 9B, upper panel) showed delayed amplification of *DpnI*-treated DNA while *MboI*-treated DNA behaved as the control. Hence, we infer that the *std* UAS is methylated in Std^{OFF} cells, in agreement with the evidence presented in Figure 9A.

(ii) DNA from Std^{ON} cells (Figure 9B, bottom panel) showed delayed amplification of both *MboI*- and *DpnI*-treated DNAs, suggesting that methylated and non-methylated GATC sites are present. Because GATC-1 appears to lie outside the HdfR binding site (Figure 7), a tentative conclusion may be that GATC-1 may be methylated and that either GATC-2 and GATC-3 or

both GATC-2 and GATC-3 may be nonmethylated in Std^{ON} cells.

DISCUSSION

The existence of epigenetic switches under DNA methylation control has been known for several decades, and a paradigm is the *pap* operon of uropathogenic *E. coli* (29,30). Additional examples include the *agn43* and *sci1* loci in *E. coli* (31–35) and the *gtr* and *opvAB* operons in *S. enterica* (36–38). In all these examples, formation of OFF and ON subpopulations is a consequence of bistable transcription, reversible ('phase-variable') or not. Another trait shared by those loci is formation of non-methylated GATC sites in regions that control transcription initiation (28,39). Non-methylation is in turn caused by GATC site occlusion and DNA methylation hindrance upon binding of transcriptional regulators to cognate regulatory regions (39,28).
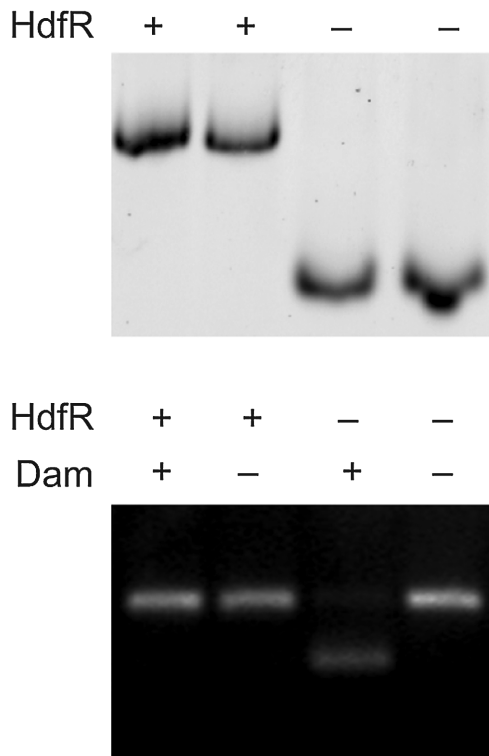
Figure 8. *In vitro* assay of DNA methylation protection by HdfR. EMSA analysis of HdfR-His$_6$ binding to a 306 bp DNA PCR product amplified from the *std* UAS (top panel). Electrophoretic separation on a 2% agarose gel of products of DNA digestion with *Dpn*I after *in vitro* methylation by Dam methylase (bottom panel).

Even though complex from a mechanistic point of view, the epigenetic switches that control bistability of the above loci are simple if compared with *std*. One complication comes from the fact that the *std* operon encodes pleiotropic regulators of transcription that activate or repress numerous genes (6). As a consequence, transition to the Std^{ON} state triggers not only cell fimbriation but additional phenotypic changes whose physiological significance remains to be fully understood (6). The speculation that these phenotypic differences may contribute to adapt Std^{OFF} and Std^{ON} subpopulations to distinct host environments may be however reasonable (6).

Another difference between *std* and other bistable loci under DNA methylation control is the sheer complexity of the mechanisms that control *std* bistability. Switching of *sci1*, *agn43*, *gtr* and *opvAB* is under the control of one main regulator (Fur or OxyR) while switching of *pap* is controlled by two main regulators, Lrp and PapI (40,29–30). In contrast, bistable expression of *std* is controlled by a network of regulators that includes StdE and StdF, two transcription factors encoded on the *std* operon itself, and HdfR, a LysR-type factor encoded outside the *std* operon. Transcription of *hdfR* is activated by StdE (Figure 3) and transcription of *std* is activated by StdF and by HdfR (Figures 2 and 4), thereby creating a complex feedback loop: StdE is necessary for HdfR synthesis and HdfR is necessary for StdE and StdF synthesis. In addition, StdF is an autogenous activator of *std* transcription.

The StdE-StdF-HdfR circuit of *std* activation is subjected to negative control by DNA adenine methylation, a trait shared with other Dam-dependent bistable switches (40). Binding of HdfR to the *std* UAS *in vitro* is hindered if GATC sites embedded in the region are methylated (Figure 6), and the *std* UAS is methylated in the Std^{OFF} cell lineage (Figure 9). In turn, the UAS of Std^{ON} cells may harbor methylated and non methylated GATC sites (Figure 9), a feature reminiscent of the regulatory patterns found in other Dam-dependent switches (28–29,39). HdfR prevents methylation of GATC-2 and GATC-3 *in vitro* (Figure 8), suggesting that formation of nonmethylated GATC sites *in vivo* may be a consequence of HdfR binding, in a fashion analogous to Dam methylation hindrance caused by other transcription factors (39),

In the model presented in Figure 10, we tentatively propose that methylation of the two promoter-proximal GATC sites (GATC-2 and GATC-3) hinders HdfR binding, thus preventing activation of the StdE-StdF-HdfR feedback loop. Because the upstream GATC site (GATC-1) appears to be dispensable for HdfR-mediated transcriptional control (Figure 7), its methylation state may not be relevant. However, this feature of the model must be considered hypothetical.

The molecular mechanisms that trigger *std* switching to the ON state remain speculative at this stage. However, a combination of experimental evidence and analogy with other Dam methylation-dependent switches may suggest the following chain of events:

(i) Low, noisy expression of the *std* operon may produce cell-to-cell variations in the amounts of StdE and StdF. In certain cells, StdE and StdF may reach a critical threshold. Above the threshold, StdE may activate *hdfR* transcription.

(ii) Activation of *hdfR* transcription by StdE may disrupt the negative feedback loop generated by autogenous repression of transcription by HdfR. As a consequence, the level of HdfR will increase, and binding of both StdF and HdfR to the UAS will activate *std* transcription. The mechanism by which HdfR overrides methylation of the *std* UAS remains unknown. However, analogy with models proposed for other Dam-dependent switches (41,42) supports the speculation that HdfR binding to the *std* UAS may occur upon UAS hemimethylation after DNA replication.

(iii) Ordinary intracellular concentration of HdfR may be sufficient to activate *std* transcription in rare cells but not to propagate the Std^{ON} state to the progeny (Figure 5, panel A). Inheritance of the Std^{ON} state is however observed upon increasing the HdfR concentration (Figure 5B). Because the intracellular concentration of HdfR is in turn dependent on StdE, the strength of the StdE-StdF-HdfR feedback loop may determine whether the Std^{ON} state is heritable or not.

The mechanism(s) that foster return from the Std^{ON} to the Std^{OFF} state remain unknown. Any signal or condition that disrupts StdE-StdF-HdfR positive feedback may be able to trigger transition to OFF, and a drop in the con-
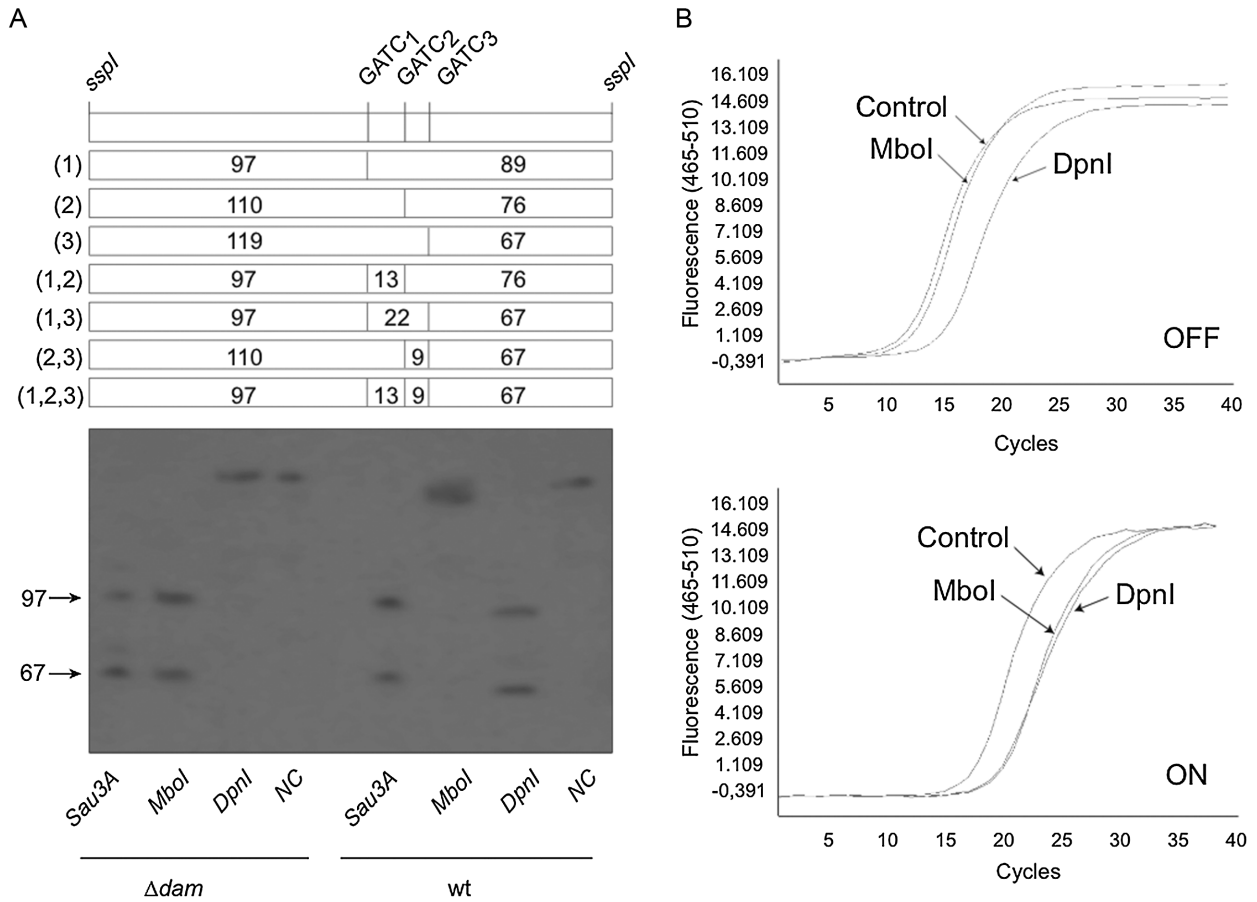
Figure 9. *In vivo* assessment of the methylation state of the GATC sites within the *std* UAS in Std[ON] and Std[OFF] subpopulations. (**A**) Southern blot of genomic DNA obtained from wild-type and non-methylated cultures, used as a control (Dam⁻), digested with *Ssp*I (control, NC) and *Dpn*I, *Mbo*I or *Sau*3AI (Bottom). (**B**) Methylation state of Std[ON] and Std[OFF] subpopulations inferred from quantitative PCR analysis after digestion with enzymes that cut GATC sequences depending on their methylation state (*Mbo*I and *Dpn*I).
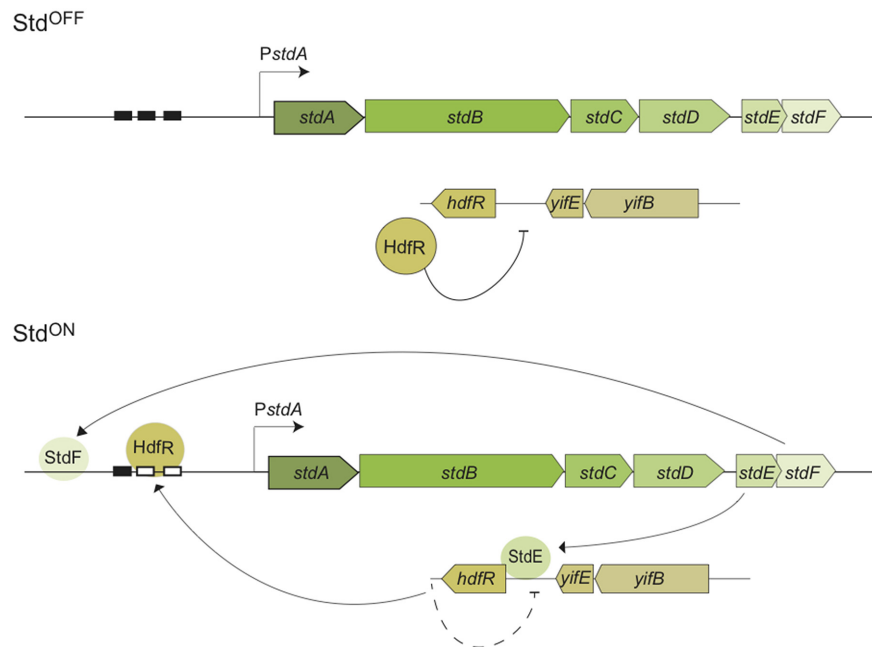

Figure 10. Model for formation of Std[OFF] and Std[ON] bacterial cell lineages. Methylated GATC sites are shown as black boxes and nonmethylated GATC sites as white boxes. The dashed line indicates that StdE-mediated disruption of autogenous *hdfR* control is hypothetical.

centration of HdfR can be expected to be crucial as it may permit methylation of the UAS.

Transcriptional control by more than one regulator can often be described by Boolean-type functions such as AND and OR logic gates (43). The regulatory mechanisms described in this study may be therefore considered a complex AND logic gate involving three regulators and an epigenetic checkpoint. Positive StdE-StdF-HdfR feedback may imbalance the system toward the Std[ON] state, while DNA adenine methylation may provide an explosion-preventing mechanism found in many bistable switches (44). In fact, lack of DNA adenine methylation locks the *std* switch in the ON state (9).

DATA AVAILABILITY

The NCBI genome assembly of *S. enterica* SL1344 was used as reference genome (NCBI GCA_000210855.2). Raw and processed data from ChIP-seq analysis have been deposited at the Gene Expression Omnibus (GEO) database (http://www.ncbi.nlm.nih.gov/geo/), with accession number GSE113562.

SUPPLEMENTARY DATA

Supplementary Data are available at NAR Online.

ACKNOWLEDGEMENTS

FUNDING

REFERENCES

1. Thanassi,D.G., Bliska,J.B. and Christie,P.J. (2012) Surface organelles assembled by secretion systems of Gram-negative bacteria: Diversity in structure and function. *FEMS Microbiol. Rev.*, **36**, 1046–1082.
2. Nuccio,S. and Bäumler,A.J. (2007) Evolution of the chaperone/usher assembly pathway: Fimbrial classification goes Greek. *Microbiol. Mol. Biol. Rev.*, **71**, 551–575.
3. Chessa,D., Winter,M.G., Jakomin,M. and Bäumler,A.J. (2009) Salmonella enterica serotype Typhimurium Std fimbriae bind terminal alpha(1,2)fucose residues in the cecal mucosa. *Mol. Microbiol.*, **71**, 864–875.
4. van der Woude,M.W. and Bäumler,A.J. (2004) Phase and antigenic variation in bacteria. *Clin. Microbiol. Rev.*, **17**, 581–611.
5. García-Pastor,L., Puerta-Fernández,E. and Casadesús,J. (2018) Bistability and phase variation in Salmonella enterica. *Biochim. Biophys. Acta*, doi:10.1016/j.bbagrm.2018.01.003.
6. García-Pastor,L., Sánchez-Romero,M.A., Gutiérrez,G., Puerta-Fernández,E. and Casadesús,J. (2018) Formation of phenotypic lineages in Salmonella enterica by a pleiotropic fimbrial switch. *PLoS Genet.*, **14**, e1007677.
7. Humphries,A.D., Raffatellu,M., Winter,S., Weening,E.H., Kingsley,R.A., Droleskey,R., Zhang,S., Figueiredo,J., Khare,S., Nunes,J. *et al.* (2003) The use of flow cytometry to detect expression of subunits encoded by 11 Salmonella enterica serotype Typhimurium fimbrial operons. *Mol. Microbiol.*, **48**, 1357–1376.
8. Balbontín,R., Rowley,G., Pucciarelli,M.G., López-Garrido,J., Wormstone,Y., Lucchini,S., García-Del Portillo,F., Hinton,J.C.D. and Casadesús,J. (2006) DNA adenine methylation regulates virulence gene expression in Salmonella enterica serovar Typhimurium. *J. Bacteriol.*, **188**, 8160–8168.
9. Jakomin,M., Chessa,D., Bäumler,A.J. and Casadesús,J. (2008) Regulation of the Salmonella enterica std fimbrial operon by DNA adenine methylation, SeqA, and HdfR. *J. Bacteriol.*, **190**, 7406–7413.
10. López-Garrido,J. and Casadesús,J. (2012) Crosstalk between virulence loci: regulation of Salmonella enterica pathogenicity island 1 (SPI-1) by products of the std fimbrial operon. *PLoS One*, **7**, e30499.
11. Hoiseth,S.K. and Stocker,B.A. (1981) Aromatic-dependent Salmonella typhimurium are non-virulent and effective as live vaccines. *Nature*, **291**, 238–239.
12. Datsenko,K.A. and Wanner,B.L. (2000) One-step inactivation of chromosomal genes in Escherichia coli K-12 using PCR products. *Proc. Natl. Acad. Sci. U.S.A.*, **97**, 6640–6645.
13. Schmieger,H. (1972) Phage P22-mutants with increased or decreased transduction abilities. *Mol. Gen. Genet.*, **119**, 75–88.
14. Garzón,A., Cano,D.A. and Casadesús,J. (1995) Role of Erf recombinase in P22-mediated plasmid transduction. *Genetics*, **140**, 427–434.
15. Bertani,G. (1951) Studies on lysogenesis. I. The mode of phage liberation by lysogenic Escherichia coli. *J. Bacteriol.*, **62**, 293–300.
16. Prieto,A.I., Ramos-Morales,F. and Casadesús,J. (2004) Bile-induced DNA damage in Salmonella enterica. *Genetics*, **168**, 1787–1794.
17. Miller,J.H. (1972) *Experiments in Molecular Genetics*. Cold Spring Harbor Laboratory Press, NY.
18. Andrews,S. (2010) FastQC: a quality control tool for high throughput sequence data. https://www.bioinformatics.babraham.ac.uk/projects/fastqc/.
19. Langmead,B., Trapnell,C., Pop,M. and Salzberg,S.L. (2009) Ultrafast and memory-efficient alignment of short DNA sequences to the human genome. *Genome Biol.*, **10**, R25.
20. Ji,H., Jiang,H., Ma,W., Johnson,D.S., Myers,R.M. and Wong,W.H. (2008) An integrated software system for analyzing ChIP-chip and ChIP-seq data. *Nat. Biotechnol.*, **26**, 1293–1300.
21. Thorvaldsdóttir,H., Robinson,J.T. and Mesirov,J.P. (2013) Integrative Genomics Viewer (IGV): high-performance genomics data visualization and exploration. *Brief. Bioinformatics*, **14**, 178–192.
22. Quinlan,A.R. and Hall,I.M. (2010) BEDTools: a flexible suite of utilities for comparing genomic features. *Bioinformatics*, **26**, 841–842.
23. Hautefort,I., Proença,M.J. and Hinton,J.C.D. (2003) Single-copy green fluorescent protein gene fusions allow accurate measurement of Salmonella gene expression in vitro and during infection of mammalian cells. *Appl. Environ. Microbiol.*, **69**, 7480–7491.
24. Lutz,R. and Bujard,H. (1997) Independent and tight regulation of transcriptional units in Escherichia coli via the LacR/O, the TetR/O and AraC/I1-I2 regulatory elements. *Nucleic Acids Res.*, **25**, 1203–1210.
25. McQuiston,J.R., Herrera-Leon,S., Wertheim,B.C., Doyle,J., Fields,P.I., Tauxe,R.V. and Logsdon,J.M. (2008) Molecular phylogeny of the salmonellae: relationships among Salmonella species and subspecies determined from four housekeeping genes and evidence of lateral gene transfer events. *J. Bacteriol.*, **190**, 7060–7067.
26. Zaim,J. and Kierzek,A.M. (2003) The structure of full-length LysR-type transcriptional regulators. Modeling of the full-length OxyR transcription factor dimer. *Nucleic Acids Res.*, **31**, 1444–1454.
27. Macián,F., Pérez-Roger,I. and Armengod,M.E. (1994) An improved vector system for constructing transcriptional lacZ fusions: Analysis of regulation of the dnaA, dnaN, recF and gyrB genes of Escherichia coli. *Gene*, **145**, 17–24.
28. Wion,D. and Casadesús,J. (2006) N6-methyl-adenine: an epigenetic signal for DNA-protein interactions. *Nat. Rev. Microbiol.*, **4**, 183–192.

29. van der Woude,M., Braaten,B. and Low,D. (1996) Epigenetic phase variation of the pap operon in Escherichia coli. *Trends Microbiol.*, **4**, 5–9.
30. Hernday,A., Krabbe,M., Braaten,B. and Low,D. (2002) Self-perpetuating epigenetic pili switches in bacteria. *Proc. Natl. Acad. Sci. U.S.A.*, **99**(Suppl. 4), 16470–16476.
31. Brunet,Y.R., Bernard,C.S., Gavioli,M., Lloubès,R. and Cascales,E. (2011) An epigenetic switch involving overlapping fur and DNA methylation optimizes expression of a type VI secretion gene cluster. *PLoS Genet.*, **7**, e1002205.
32. Henderson,I.R., Meehan,M. and Owen,P. (1997) Antigen 43, a phase-variable bipartite outer membrane protein, determines colony morphology and autoaggregation in Escherichia coli K-12. *FEMS Microbiol. Lett.*, **149**, 115–120.
33. Henderson,I.R. and Owen,P. (1999) The major phase-variable outer membrane protein of Escherichia coli structurally resembles the immunoglobulin A1 protease class of exported protein and is regulated by a novel mechanism involving Dam and oxyR. *J. Bacteriol.*, **181**, 2132–2141.
34. Haagmans,W. and van der Woude,M. (2000) Phase variation of Ag43 in Escherichia coli: Dam-dependent methylation abrogates OxyR binding and OxyR-mediated repression of transcription. *Mol. Microbiol.*, **35**, 877–887.
35. Waldron,D.E., Owen,P. and Dorman,C.J. (2002) Competitive interaction of the OxyR DNA-binding protein and the Dam methylase at the antigen 43 gene regulatory region in Escherichia coli. *Mol. Microbiol.*, **44**, 509–520.
36. Broadbent,S.E., Davies,M.R. and van der Woude,M.W. (2010) Phase variation controls expression of Salmonella lipopolysaccharide modification genes by a DNA methylation-dependent mechanism. *Mol. Microbiol.*, **77**, 337–353.
37. Cota,I., Sánchez-Romero,M.A., Hernández,S.B., Pucciarelli,M.G., García-Del Portillo,F. and Casadesús,J. (2015) Epigenetic control of salmonella enterica o-antigen chain length: a tradeoff between virulence and bacteriophage resistance. *PLoS Genet.*, **11**, e1005667.
38. Cota,I., Bunk,B., Spröer,C., Overmann,J., König,C. and Casadesús,J. (2016) OxyR-dependent formation of DNA methylation patterns in OpvABOFF and OpvABON cell lineages of Salmonella enterica. *Nucleic Acids Res.*, **44**, 3595–3609.
39. Casadesús,J. and Low,D. (2006) Epigenetic gene regulation in the bacterial world. *Microbiol. Mol. Biol. Rev.*, **70**, 830–856.
40. Sánchez-Romero,M.A., Cota,I. and Casadesús,J. (2015) DNA methylation in bacteria: from the methyl group to the methylome. *Curr. Opin. Microbiol.*, **25**, 9–16.
41. Kaminska,R. and van der Woude,M.W. (2010) Establishing and maintaining sequestration of Dam target sites for phase variation of agn43 in Escherichia coli. *J. Bacteriol.*, **192**, 1937–1945.
42. Hernday,A.D., Braaten,B.A. and Low,D.A. (2003) The mechanism by which DNA adenine methylase and PapI activate the pap epigenetic switch. *Mol. Cell*, **12**, 947–957.
43. Silva-Rocha,R. and de Lorenzo,V. (2008) Mining logic gates in prokaryotic transcriptional regulation networks. *FEBS Lett.*, **582**, 1237–1244.
44. Wilhelm,T. (2009) The smallest chemical reaction system with bistability. *BMC Syst. Biol.*, **3**, 90.